Cell PRESS
Cancer Cell
Article

Englerin A Stimulates PKCθ to Inhibit Insulin Signaling and to Simultaneously Activate HSF1: Pharmacologically Induced Synthetic Lethality

Carole Sourbier,[1] Bradley T. Scroggins,[1] Ranjala Ratnayake,[3] Thomas L. Prince,[1] Sunmin Lee,[2] Min-Jung Lee,[2] Peter Literati Nagy,[4] Young H. Lee,[1] Jane B. Trepel,[2] John A. Beutler,[3] W. Marston Linehan,[1] and Len Neckers[1,*]
[1]Urologic Oncology Branch
[2]Medical Oncology Branch
Center for Cancer Research, National Cancer Institute, National Institutes of Health, Bethesda, MD 20892, USA
[3]Molecular Targets Laboratory, Center for Cancer Research, National Cancer Institute, Frederick, MD 21702, USA
[4]N-Gene Research Laboratories, Inc., 1137 Budapest, Hungary
*Correspondence: neckersl@mail.nih.gov
http://dx.doi.org/10.1016/j.ccr.2012.12.007

SUMMARY

The natural product englerin A (EA) binds to and activates protein kinase C-θ (PKCθ). EA-dependent activation of PKCθ induces an insulin-resistant phenotype, limiting the access of tumor cells to glucose. At the same time, EA causes PKCθ-mediated phosphorylation and activation of the transcription factor heat shock factor 1, an inducer of glucose dependence. By promoting glucose addiction, while simultaneously starving cells of glucose, EA proves to be synthetically lethal to highly glycolytic tumors.

INTRODUCTION

Many solid tumors are characterized by an altered metabolic program and display increased dependence on glucose. Several signaling pathways and transcription factors are critical for providing sustained intake of glucose by tumor cells and for enforcing their glycolytic dependence, including the insulin signaling pathway (Leto and Saltiel, 2012) and the heat shock transcription factor heat shock factor 1 (HSF1) (Dai et al., 2007). Whereas a lack of function of the insulin pathway or HSF1 has been linked to diabetes and aging, hyperinsulinemia and HSF1 activation have been linked to the development of cancer (Whitesell and Lindquist, 2009; Gallagher and LeRoith, 2011; Mendillo et al., 2012). Indeed, recent reports suggest that dependence on HSF1 reflects the "nononcogene addiction" of tumor cells for this transcription factor (Solimini et al., 2007).

Molecular mechanisms underlying HSF1-enforced glucose dependence are not well understood. However, effects of the insulin pathway on glucose uptake and utilization have been well characterized. Insulin and insulin-like growth factors activate the PI3K/AKT pathway to stimulate glucose uptake. Numerous epithelial tumors rely on constitutive activation of this pathway to increase their supply of glucose (Vander Heiden et al., 2009; Leto and Saltiel, 2012). The protein kinase C (PKC) family of kinases exerts both positive and negative effects on this pathway (Nelson et al., 2008). In type II diabetes, activation of some PKCs, including PKCθ, with fatty acids or diacylglycerol can induce insulin resistance via inhibitory phosphorylation of insulin receptor substrate 1 (IRS1) (Griffin et al., 1999; Li et al., 2004). Phosphorylated IRS1 dissociates from the insulin receptor, leading to decreased signaling via PI3K/AKT and reduced glucose uptake (Li et al., 2004; Griffin et al., 1999).

PKC isozymes are divided into three groups: conventional PKCs (PKCα, PKCβI, PKCβII, and PKCγ), novel PKCs (PKCδ, PKCθ, PKCε, and PKCη), and atypical PKCs (PKCζ and PKCι). Although PKCα, -δ, and -ε are broadly expressed, other isozymes have a more restricted expression. For example, PKCθ is mainly expressed in T lymphocytes and in some tumors (Marsland and Kopf, 2008; Griner and Kazanietz, 2007). Because of the lack of selectivity of available PKC modulators, the role played by each isozyme in tumorigenesis is not well understood (Griner and Kazanietz, 2007).

Significance

Many epithelial tumors display a glycolytic phenotype characterized by enhanced dependence on glucose. Targeting the abnormal metabolism of such tumors has been a long-term goal of the scientific community. The natural product EA selectively activates PKCθ to induce a metabolic catastrophe in glycolytic tumor cells by promoting insulin resistance and inhibiting glucose uptake, while simultaneously activating the heat shock transcription factor HSF1, thereby enforcing glucose dependence. These data identify EA as a mechanistically unique cytotoxic agent.

Table 1. EA Cytotoxicity Correlates with Glucose Sensitivity in a Panel of Cell Lines

Cell line	Origin of the tissue	EA (IC_{50})	2-DG (IC_{50})
786-0	Kidney cancer ($VHL^{-/-}$) (Williams et al., 1978)	50 nM	60 μM
786-0/VHL	VHL-restored cell line (Tong et al., 2011)	>10 μM	>1 mM
UOK257	Kidney cancer ($FLCN^{-/-}$) (Yang et al., 2008)	65 nM	285 μM
UOK257WT	FLCN-restored cell line (Hong et al., 2010)	>10 μM	721 μM
UOK262	Kidney cancer metastasis ($FH^{-/-}$) (Yang et al., 2010)	35 nM	222 μM[a]
UOK262WT	FH-restored cell line (Tong et al., 2011)	>10 μM	>1 mM[a]
HK2	Normal kidney (proximal tubule) (Ryan et al., 1994)	>10 μM	>1 mM
HEK293	Embryonic epithelial kidney cell (Pear et al., 1993)	>10 μM	>1 mM
PC3	Prostate cancer (Kaighn et al., 1979)	5 μM	300 μM
SKBr3	Breast cancer (Fogh and Trempe, 1975)	3 μM	n/a

Cells (70% confluence) were treated with a range of EA concentrations (1 nM–10 μM) in serum-free media. After 48 hr, viability was measured by MTT or manual cell counting. For UOK262 and UOK262WT, viability was only assessed by manual cell counting. Molecularly restored kidney cancer cell lines and normal kidney cell lines did not show significant sensitivity toward EA. Glucose dependence of the cells was similarly assessed by determining sensitivity to 2-deoxyglucose (2-DG, 10 nM−100 μM). Cells were cultured in DMEM containing 1g/l glucose and were treated with 2-DG for 72 hr (786-0, 786-0/VHL, UOK257, UOK257WT, HK2, HEK293, PC3, and SKBr3), [a]except for UOK262 and UOK262WT, which were treated for 24 hr. Viability was assessed by MTT and/or manual cell counting as above. EA sensitivity displays a highly significant positive correlation with glucose dependence, as assessed by determining R^2 and the Pearson Correlation Coefficient (R^2 = 0.9126; Pearson Correlation Coefficient = 0.962; p = 0.000003). UOK262 data were not included when determining R^2 and the Pearson Correlation Coefficient because they were exposed to 2-DG for 24 hr and not 72 hr like the other cell lines.

The epoxyguaiane englerin A (EA) is a natural product that displays selective in vitro cytotoxicity toward kidney cancer cell lines in the NCI-60 cell line panel (Ratnayake et al., 2009). Because EA's cytotoxicity profile suggests a unique mechanism of action, we sought to identify EA's molecular target(s) in order to provide potentially novel therapeutic anticancer strategies.

RESULTS

EA Is Selectively Cytotoxic for a Panel of Genetically Defined Kidney Cancer Cell Lines

Using cell lines derived from three genetically defined kidney cancers (Clear Cell Renal Cell Cancer, 786-0; Hereditary Leiomyomatosis Renal Cell Cancer, UOK262; Birt-Hogg-Dubé Syndrome, UOK257) and their molecularly restored (e.g., stable re-expression of VHL, FH, or Folliculin, respectively; see references in Table 1) nontumorigenic isogenic counterparts, we assessed EA cytotoxicity by MTT assay and/or manual cell counting (Table 1). Whereas the three genetically defined kidney cancer cell lines displayed an IC_{50} for EA of 35–50 nM, in each case the molecularly restored isogenic counterpart was markedly less sensitive to EA (IC_{50} > 10 μM). Two nontumorigenic kidney-derived cell lines, HK2 and HEK293, were similarly insensitive to EA (IC_{50} > 10 μM). In contrast, the prostate cancer cell line PC3 and the breast cell line SKBr3 displayed intermediate sensitivity to EA (IC_{50} = 3–5 μM). Sensitivity to EA correlated significantly with sensitivity to 2-deoxyglucose (2-DG), an indicator of glucose dependence (Table 1).

EA Selectively Activates PKCθ

Because nothing is known about EA's mechanism of action, we predicted potential target(s) by structure activity relationship analysis (see the Experimental Procedures). Fifteen potential molecular targets were identified, half of which were isoforms of protein kinase C (PKC) (Table S1 available online). Therefore, we investigated further the potential effect of EA on PKCs, first using a pan-PKC kinase assay. We found that treatment of whole-cell extracts with EA increased pan-PKC activity in a dose-dependent manner (Figure 1A; Figure S1). To identify which PKC isoforms were responsive to EA, we individually silenced expression of PKC-α, -δ, -θ, -η, or -ε in 786-0 cells and examined the impact on EA cytotoxicity. Only PKCθ knockdown abrogated EA cytotoxicity (Figure 1B), suggesting that PKCθ may be a target of EA. We confirmed this hypothesis by evaluating the effect of EA on the enzymatic activity of purified PKCθ in vitro. We found that PKCθ-mediated phosphorylation of its substrate IRS1 was dose-dependently enhanced by EA (Figures 1C and 1D).

Because PKCθ is structurally very similar to PKCδ, we asked whether EA's effect on PKC activity is due solely to PKCθ activation. Phorbol esters, including the fluorescent analog sapintoxin D (SAPD), bind to the same pocket in PKCs as does diacylglycerol (DAG) and are well-known PKC activators. Unlike PKCθ and PKCδ, conventional PKCs, including PKCα, require priming with Ca^{2+} in order to bind either DAG or phorbol esters (Luo and Weinstein, 1993; Griner and Kazanietz, 2007). In vitro kinase assay (in the absence of Ca^{2+}) using either PKCα, -δ, or -θ proteins confirmed that EA selectively activates PKCθ. In contrast, SAPD activated both PKCδ and PKCθ under the same assay conditions (Figure 1E).

Finally, we took advantage of the fluorescent properties of SAPD to confirm the binding of EA to PKCθ (Figure 1F). Purified PKCθ was incubated for 20 min with EA (1 μM) or DMSO prior to the addition of SAPD (2 μM). We found that premixing PKCθ with EA significantly reduced SAPD binding, supporting the hypothesis that EA interacts with a motif in PKCθ, either contiguous with or close to the SAPD/DAG binding domain. Premixing EA with PKCδ had no effect on SAPD binding (data not shown).

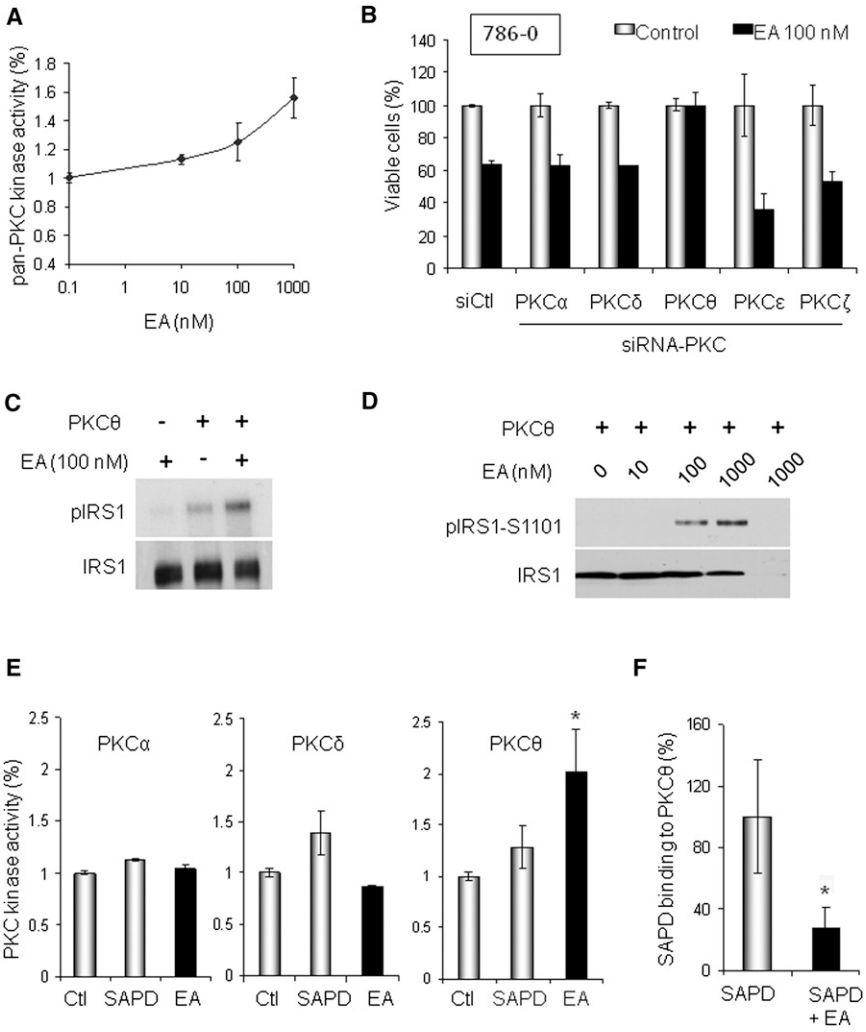

Figure 1. EA Is a Selective PKCθ Activator

(A) Pan-PKC kinase activity was assessed in 786-0 cells following EA treatment. Whole-cell lysates were incubated for 1 hr at 30°C with EA or DMSO in the presence of ATP (10 μM). PKC kinase activity was quantified by spectrophotometry (see the Experimental Procedures).

(B) Viability (determined by MTT assay) after 24 hr EA treatment (100 nM) of 786-0 cells silenced for different PKC isoforms by RNA interference.

(C) Effect of 30 min EA (100 nM) treatment on PKCθ-mediated phosphorylation of IRS1. A radioactive kinase activity assay was performed in the presence of 6 μCi (0.2 μM) of [^{32}P]-ATP and 10 μM nonradioactive ATP using purified PKCθ (50 ng) and its substrate IRS1 (50 ng).

(D) Nonradioactive dose-dependent effects of EA on PKCθ-mediated phosphorylation of IRS1-S1101 using purified proteins were assessed by immunoblotting (1 hr treatment; 10 ng PKCθ, 20 ng IRS1). The last lane omits IRS1 and is a negative control.

(E) Purified PKCα, PKCδ, or PKCθ (5 ng) were incubated for 1 hr with DMSO, SAPD (2 μM), or EA (1 μM) in presence of ATP (10 μM). PKC kinase activity was quantified by spectrophotometry.

(F) EA competes with the fluorescent phorbol ester SAPD for binding to PKCθ. EA (1 μM) was preincubated for 20 min with 5 ng purified PKC protein prior to addition of SAPD (2 μM). SAPD fluorescence shifts from 455 nm to 420 nm when it is bound to PKC. Thus, fluorescence emission was measured at 420 nm (excitation at 355 nm) to assess SAPD binding in presence or absence of EA (*$p < 0.05$). Data are displayed as the mean ± SD (see also Figure S1 and Table S1).

PKCθ Activation Induces an Insulin-Resistant Phenotype in Tumor Cells

Because we demonstrated that EA enhanced PKCθ-mediated inhibitory phosphorylation of IRS1 (on S1101) in vitro, we hypothesized that EA might induce an insulin-resistant phenotype. EA enhanced the inhibitory phosphorylation of IRS1 in 786-0 cells and led to reduced activating phosphorylations of AKT (T308 and S473) and reduced AKT-mediated phosphorylation of GSK3β (S9). These effects are PKCθ-dependent because they were ameliorated upon siRNA-mediated silencing of PKCθ (Figure 2A). EA also reduced glucose uptake in 786-0 cells, to a similar degree as the Glut1 inhibitor fasentin (Figure 2B), and decreased cellular ATP content as well (Figure 2C). However, at the concentration used, fasentin only slightly affected 786-0 cell viability (Figure S2A), whereas addition of cell permeable pyruvate (methylpyruvate) abrogates EA cytotoxicity (Figure S2B). These data suggest that glucose uptake inhibition contributes to but does not solely account for EA cytotoxicity.

Next, we assessed the role played by insulin pathway inhibition in EA-mediated inhibition of AKT. We confirmed that the inhibitory effect of EA on AKT activity was IRS1-dependent because EA-mediated AKT inhibition was overcome by the inclusion of EGF in the culture media (Figure S2C). To confirm the importance of IRS1-dependent AKT inhibition for EA cytotoxicity, we infected 786-0 cells with several AKT viral constructs. As shown in Figure 2D (upper panel), expression of dominant negative AKT (AktDN) enhanced EA cytotoxicity, whereas expression of constitutively active AKT (AktCA) protected cells from EA. These impacts on EA cytotoxicity were consistent with AKT activity status (Figure 2D, lower panel; Figure S2D), and the data clearly implicate IRS1-dependent inhibition of AKT as a necessary component of the cytotoxic response to EA.

To determine whether the in vitro cytotoxicity of EA was obtainable in vivo, we treated athymic mice bearing 786-0 tumor xenografts with EA (5 mg/kg intraperitoneally, daily except Sunday). EA markedly inhibited tumor growth during the 2-week treatment period (Figure 2E). In agreement with our in vitro data, inhibitory phosphorylation of IRS1 was increased, and activity of the PI3K/AKT pathway was decreased in 786-0 tumors excised from mice treated with EA, when compared to tumors from vehicle-treated mice (Figure 2F). Importantly, in a second tumor xenograft model, EA inhibited human prostate tumor growth by up to 60% (Figure S2E), consistent with its

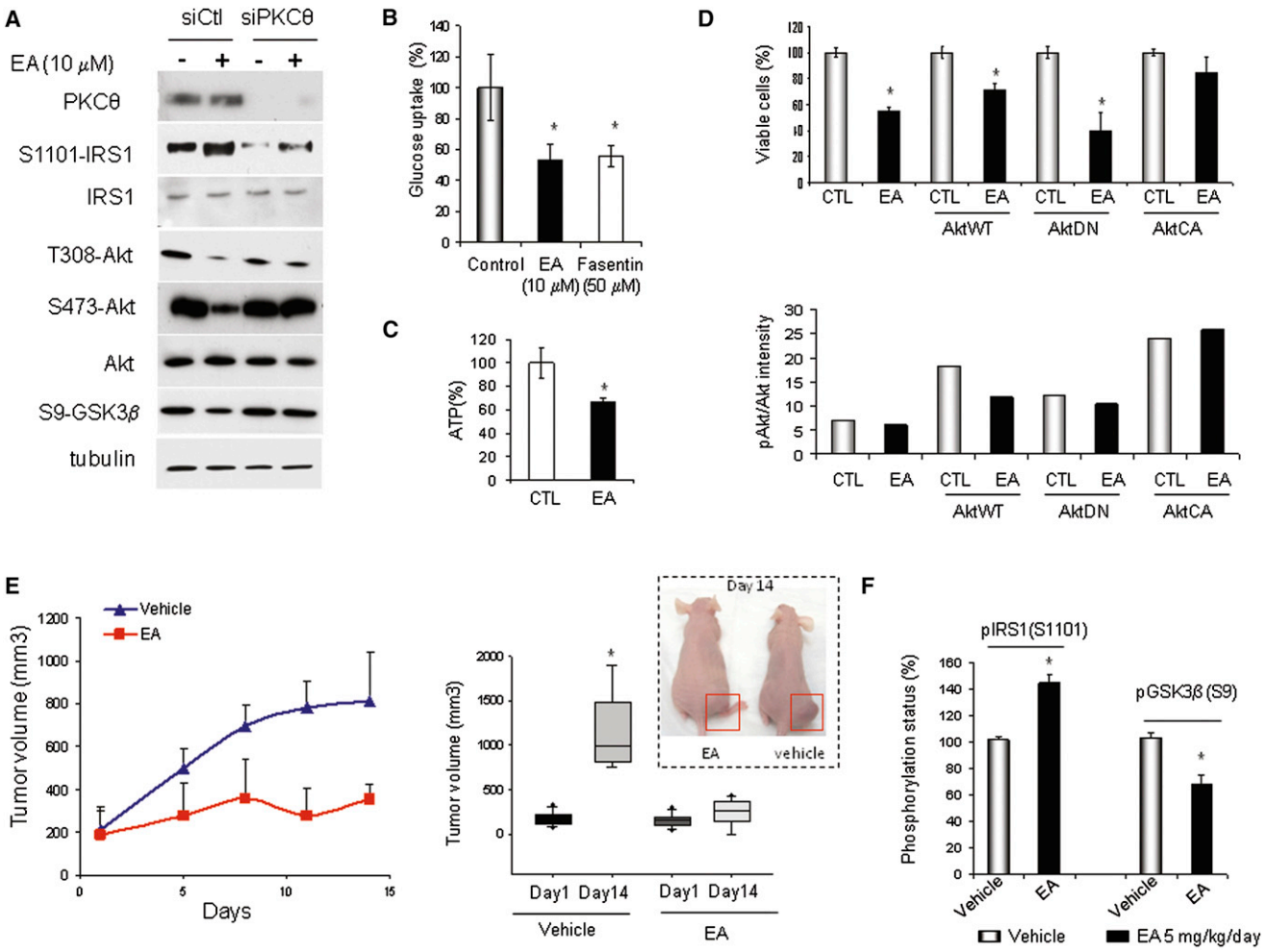

Figure 2. EA Induces Insulin Resistance In Vitro and In Vivo

(A) EA-mediated phosphorylation of IRS1 (S1101), AKT (pT308 and pS473), and GSK3β (pS9) in 786-0 cells requires PKCθ expression. EA treatment (10 μM) was for 6 hr.

(B) EA inhibits glucose uptake in 786-0 cells as shown by using the nondegradable fluorescent glucose analog 2-NBDG. The Glut1 inhibitor fasentin (50 μM) is shown as a positive control. EA and fasentin treatments were for 3 hr.

(C) Effect of EA treatment (6 hr, 1 μM) on ATP levels in 786-0 cells was measured using ATPlite assay.

(D) Effect of AKT activation on EA cytotoxicity. 786-0 cells were infected 24 hr prior to EA treatment with AKT lentiviral constructs: wild-type AKT (AktWT), dominant negative AKT (AktDN), or constitutively active AKT (AktCA). After treatment with 1 μM EA for an additional 24 hr, cell viability was assessed by manual cell counting with trypan blue exclusion (upper panel). Impact of lentiviral infections on AKT activity is shown in the lower panel and in Figure S2D. EA inhibits the activity of wild-type but not of constitutively active AKT.

(E) Effect of EA treatment (5 mg/kg, daily except Sunday) on xenograft growth of 786-0 cells in athymic mice (vehicle: PBS/DMSO, 1/1). The left panel displays the growth curve of one of two animal experiments, each with eight animals per group. The right panel represents the averaged mean end point tumor volumes of the two experiments (32 animals in total).

(F) EA treatment in vivo stimulates inhibitory phosphorylation of IRS1 (pS1101) and reduced phosphorylation of the AKT substrate GSK3β (pS9) in tumor xenografts of treated mice. *$p < 0.05$. Data are displayed as the mean ± SD (see also Figure S2).

ability to stimulate PKCθ in these cells and with its in vitro toxicity profile (Figure S1; Table 1).

PKCθ Induces Heat-Shock-Independent Activation of HSF1

Because the in vivo data support further evaluation of EA as an anticancer agent, we asked whether treated animals might develop hyperglycemia because of induction of systemic insulin resistance. We measured blood glucose level in mice harboring either 786-0 or PC3 xenografts before and following a single treatment with either EA or vehicle (PBS/DMSO, 1:1). Surprisingly, mice treated with EA displayed significantly lower blood glucose compared to vehicle-treated mice (Figure 3A).

Chemically induced reduction in blood glucose has been reported previously and is thought to be due to increased HSP70, resulting in sensitization of cells to insulin (Chung et al., 2008; Kavanagh et al., 2011). We observed that in mice treated with EA both plasma and tumor HSP70 were elevated

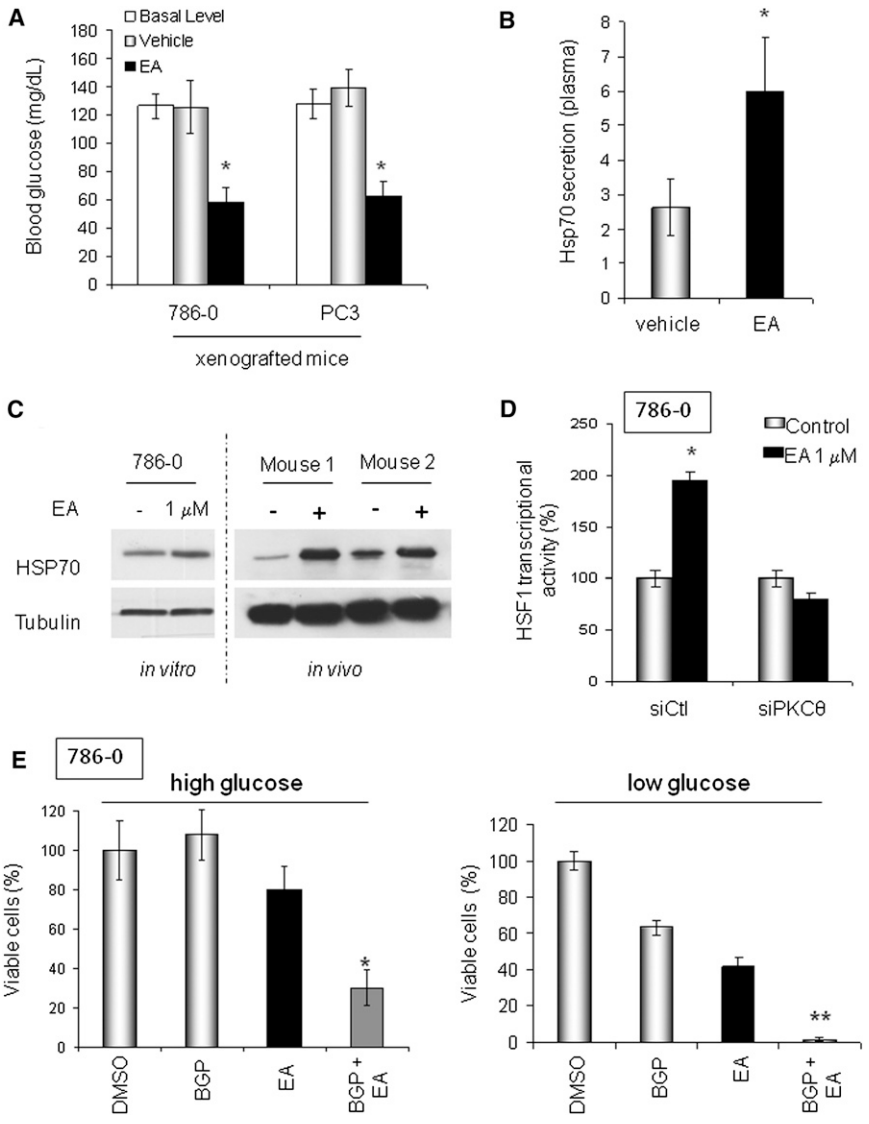

Figure 3. EA Activates HSF1

(A) Effect of EA on blood glucose level in tumor-bearing mice prior to ("basal level") or 5 min after treatment with EA (EA, 5 mg/kg; vehicle: PBS/DMSO, 1/1).

(B) Quantification of plasma HSP70 level in tumor-bearing mice 4 hr following EA treatment (EA: 5 mg/kg; vehicle: PBS/DMSO, 1/1).

(C) HSP70 protein expression following EA treatment of 786-0 cells in vitro (EA, 1 μM for 8 hr) and in vivo (786-0 xenografts; prior to and 8 hr after EA, 5 mg/kg) was assessed by immunoblotting.

(D) EA stimulation of HSF1 transcriptional activity requires PKCθ expression. HSF1 activity was measured in cells transiently transfected with a *HSP70 HSE*-promoter *GFP*-tagged reporter plasmid 6 hr after EA treatment.

(E) EA cytotoxicity is affected by HSF1 activation and extracellular glucose concentration. BGP-15 prolongs the HSF1 transcriptional response. High glucose medium contains 4.5 g/l glucose; low glucose medium contains 1 g/l glucose. BGP-15 was used at 50 μM (Chung et al., 2008) and EA was used at 1 μM. Incubation was for 24 hr. Viability was assessed by MTT assay and confirmed by manual cell counting of trypan blue-excluding cells using a hemacytometer. *$p < 0.05$; **$p < 0.001$. Data are displayed as the mean ± SD (see also Figure S3).

compared to vehicle-treated mice (Figures 3B and 3C). HSP70 is a marker of cell stress and is a transcriptional target of HSF1 (Trepel et al., 2010). Consistent with these data, we observed that EA induced HSF1 nuclear translocation and upregulated its transcriptional activity in a PKCθ-dependent manner (Figures 3D and S3).

Because HSF1 has recently been identified as a contributing factor for tumorigenesis and likely represents a nononcogene addiction of most tumor cells (Whitesell and Lindquist, 2009; Santagata et al., 2011; Dai et al., 2007; Mendillo et al., 2012; Min et al., 2007), we investigated whether HSF1 activation might compromise EA cytotoxicity, much as it is thought to compromise the cytotoxicity of HSP90 inhibitors (which also induce HSF1 [Zou et al., 1998]). We examined the impact of the HSF1 chemical enhancer BGP-15, currently under clinical evaluation for treating insulin-resistance disorders (Chung et al., 2008; Literáti-Nagy et al., 2009; Hargitai et al., 2003), on EA-induced cytotoxicity. To our surprise, addition of BGP-15 significantly increased EA cytotoxicity (Figure 3E, left panel). We have shown that PKCθ induced insulin resistance in tumor cells, and Dai et al. (2007) demonstrated that HSF1 enforces glucose dependence in tumor cells. Thus, we hypothesized that the increased cytotoxicity obtained in vitro upon combination of BGP-15 and EA might result from the simultaneous occurrence of these two metabolic events. If this were the case, the cytotoxicity of an EA/ BGP-15 drug combination should be augmented in cells exposed to low glucose. Indeed, as shown in Figure 3E (right panel), BGP-15 and EA, either administered as individual agents or in combination, displayed greater cytotoxicity when tumor cells were cultured in low glucose media.

EA Cytotoxicity Requires Expression of Both PKCθ and HSF1

Next, we asked whether HSF1 expression is necessary for EA-induced cytotoxicity. Using shRNA to knock down HSF1 (Figure S4A), we found that HSF1 expression, like PKCθ, is essential for cell sensitivity to EA (Figure 4A). Importantly, the synergistic effect obtained by combining BGP-15 and EA (see Figure 3E) also depended on HSF1 expression. To provide further support for our hypothesis that both PKCθ and HSF1 are necessary for EA cytotoxicity, we made use of the fact that HEK293 cells are insensitive to EA (see Table 1), express undetectable levels of endogenous PKCθ, and do not overexpress HSF1 (data not shown). We were able to induce EA sensitivity in HEK293 cells after transfection with both PKCθ and HSF1 but not after

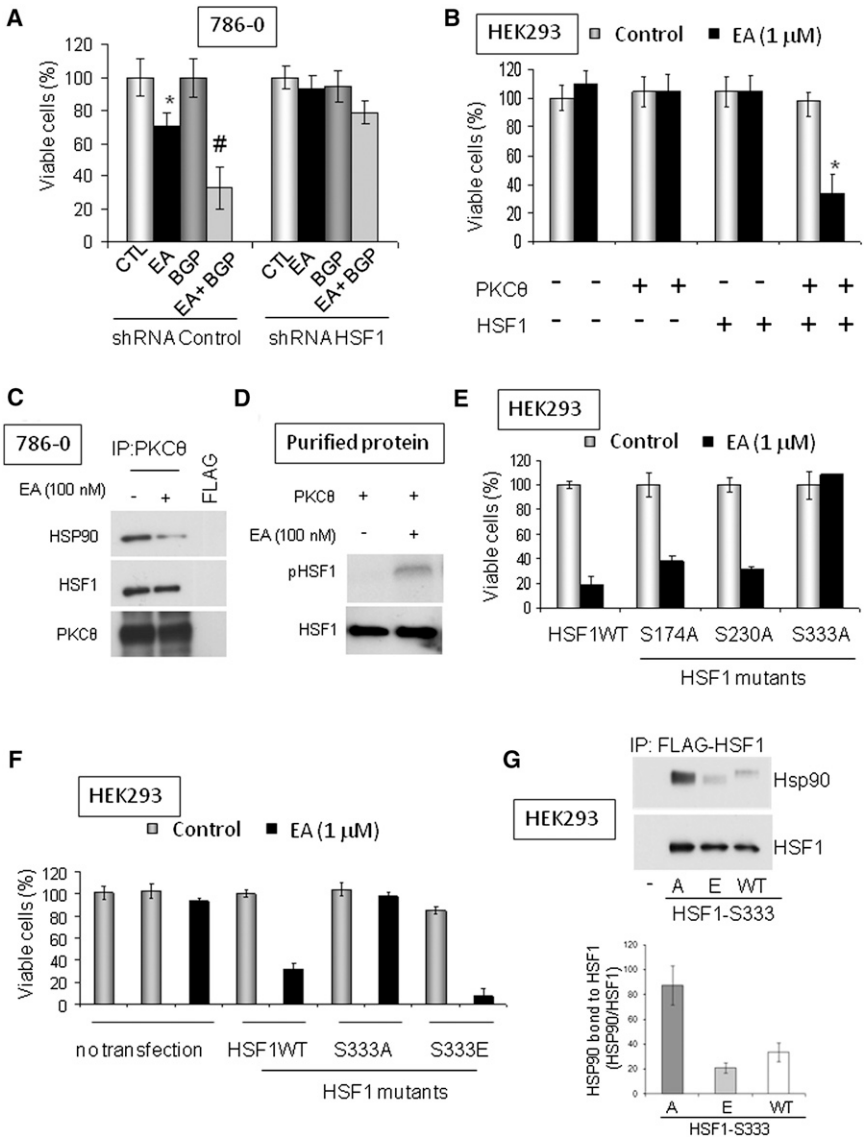

Figure 4. PKCθ and HSF1 Are Both Necessary for EA Cytotoxicity in Tumor Cells

(A) EA sensitivity of 786-0 cells to EA and EA/BGP-15 requires HSF1 expression. EA was used at 1 μM and BGP-15 at 50 μM (24 hr). HSF1 expression was decreased by transfection of HSF1-specific shRNA 24 hr prior to treatment. *$p < 0.05$ (compared to control); #, $p < 0.05$ (compared to EA-treated).

(B) HEK293 cells are not sensitive to EA. HSF1 and PKCθ overexpression confers EA sensitivity on HEK293 cells (EA treatment was for 24 hr at 1 μM, commencing 24 hr after transfection). *$p < 0.05$ (compared to cotransfected control).

(C) Interaction of endogenous HSF1 and PKCθ in 786-0 cells was visualized by immunoprecipitation of endogenous PKCθ and blotting for associated HSF1. 786-0 cells grown in 6-well plates were lysed in TNESV buffer. The lysates were treated for 1 hr with EA (100 nM) or DMSO at 30°C before immunoprecipitation. HSP90 interaction with the PKCθ/HSF1 immunocomplex was reduced by EA treatment (left panel). The inputs for this experiment can be found in Figure S4C.

(D) EA stimulates PKCθ-mediated phosphorylation of purified HSF1 in vitro (50 ng of purified proteins; treatment for 30 min at 30°C).

(E) Identification of a putative PKCθ phosphorylation site on HSF1. HEK293 cells were transfected with PKCθ and either wild-type or point mutated HSF1 plasmids (see Figures S4E and S4F) and sensitivity to EA was assessed (treatment for 24 hr with 1 μM EA).

(F) Effect of HSF1 S333 mutants on EA sensitivity of HEK293 cells overexpressing PKCθ. The phosphomimetic mutant HSF1-S333E supports EA cytotoxicity, whereas the nonphosphorylatable mutant HSF1-S333A does not (treatment for 24 hr with 1 μM EA).

(G) Association of HSF1-S333A, HSF1-S333E, and wild-type HSF1 with HSP90. HEK293 cells were transiently transfected with Flag-tagged HSF1 plasmids as indicated. After 24 hr, Flag immunoprecipitates were subjected to SDS-PAGE, transferred to PVDF membrane, and immunoblotted for associated endogenous HSP90. Anti-HSF1 antibody was also blotted to monitor the uniformity of HSF1 expression and efficiency of immunoprecipitation. The phosphomimetic mutant HSF1-S333E associates with endogenous HSP90 to a markedly lesser degree than does nonphosphorylatable HSF1-S333A; HSP90 association with wild-type HSF1 is shown for comparison. Band optical densities from two separate experiments were obtained by image analysis software and the HSP90 band density in each case was normalized to the respective HSF1 band density (graphical insert). The inputs for this experiment can be found in Figure S4H. Data are displayed as the mean ± SD (see also Figure S4).

transfection with either construct alone (Figure 4B; see Figure S4B for inputs).

Extending our observation that PKCθ is necessary for HSF1 activation by EA (Figure 3D), we were able to detect the interaction of endogenous PKCθ and HSF1 in 786-0 cells (Figure 4C; see Figure S4C for inputs). In addition, we found that PKCθ phosphorylated HSF1 in vitro in the presence of EA (Figure 4D), and EA-induced serine phosphorylation of endogenous HSF1 in 786-0 cells was PKCθ-dependent (Figure S4D). Further, we observed that HSP90 was also a component of the HSF1/PKCθ complex but was dissociated after treatment with EA (Figure 4C).

Because dissociation from HSP90 is a prerequisite for HSF1 activation (Anckar and Sistonen, 2011; Zou et al., 1998), these data suggest that PKCθ phosphorylation of HSF1 may promote this process. To identify a putative PKCθ phosphorylation site(s) on HSF1, we mutated several predicted PKC consensus phosphorylation sites (see Figure S4E), and we examined the ability of these HSF1 mutants to complement exogenous PKCθ in mediating EA cytotoxicity in HEK293 cells (Figure 4E; see Figure S4F for inputs). EA cytotoxicity was abrogated only when HSF1 serine 333 was mutated to alanine (S333A), implicating S333 as a potential PKCθ phosphorylation site. Supporting this possibility, we found that the phosphomimetic mutant HSF1-S333E, but not the nonphosphorylatable mutant HSF1-S333A, fully complemented PKCθ-dependent EA cytotoxicity (Figure 4F; see Figure S4G for inputs).

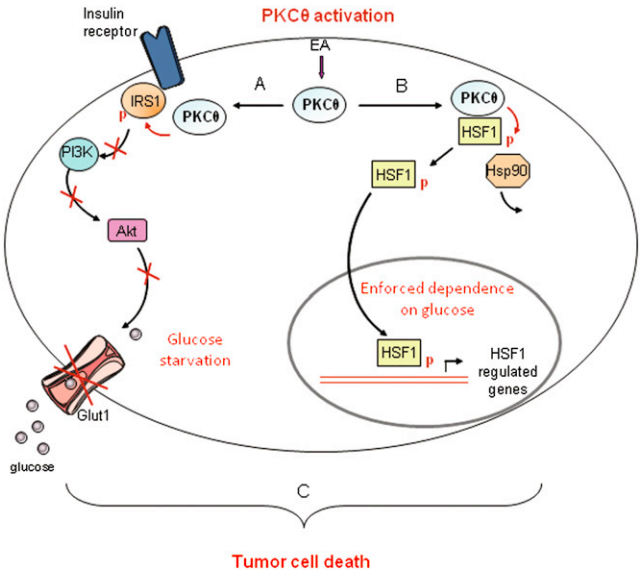

Figure 5. EA Proposed Mechanism of Action: Activation of PKCθ in Cells Expressing HSF1 Leads to Simultaneous Induction of Insulin Resistance and Glucose Dependence, Resulting in Metabolic Catastrophe

(A) EA-dependent activation of PKCθ stimulates an insulin-resistant phenotype via inhibitory phosphorylation of IRS1 and inhibition of AKT, limiting access of tumor cells to glucose.

(B) EA simultaneously stimulates PKCθ-mediated phosphorylation and activation of HSF1, a transcription factor that enforces tumor cell glucose dependence (Dai et al., 2007).

(C) By simultaneously inducing insulin resistance and glucose dependence, EA is synthetically lethal to glycolytic tumor cells.

Although the domain of HSF1 that interacts with HSP90 is not known, S333 is located within the regulatory domain of the transcription factor, a region rich in posttranslational modification sites and important for the stress inducibility of HSF1 (Anckar and Sistonen, 2011). Therefore, we examined whether S333 mutation to either alanine or glutamic acid affected HSF1 interaction with HSP90. FLAG-tagged HSF1 wild-type, S333A, and S333E plasmids were transiently transfected into HEK293 cells, and FLAG immunoprecipitates were probed for associated endogenous HSP90. Indeed, we found that HSF1-S333A associated with endogenous HSP90 to a markedly greater extent than did HSF1-S333E (Figure 4G; see Figure S4H for inputs). These data are consistent with the hypothesis that PKCθ-mediated phosphorylation of HSF1 S333 promotes dissociation from HSP90. Supporting this possibility, we found that HSF1-S333E was more efficiently activated (>2-fold) by heat shock when compared to HSF1-S333A (Figure S4I).

DISCUSSION

Survival of tumor cells depends on their ability to adapt to their environment. Because cellular transformation is associated with an increased dependence on glucose (Vander Heiden et al., 2009), tumor cells have reprogrammed their cellular signaling pathways to allow for increased glucose uptake. Indeed, positron emission tomography with 2-deoxy-2(^{18}F)-fluoro-D-glucose, a nonmetabolizable glucose analog, is frequently used to distinguish tumors from adjacent normal tissues (Gambhir, 2002), and targeting glucose uptake and/or metabolism has been explored for its therapeutic potential in treating cancer, including VHL-deficient kidney cancer (Chan et al., 2011; Hamanaka and Chandel, 2012). The insulin pathway and the transcription factor HSF1 are two examples of evolutionarily conserved signaling networks that support and foster the glucose dependence of tumor cells (Barbieri et al., 2003; Pirkkala et al., 2001; Dai et al., 2007).

In this study, we have identified a unique strategy to create metabolic disaster in glucose-dependent tumor cells by selectively activating PKCθ with the natural product EA (schema illustrated in Figure 5). When examined in a panel of kidney-cancer-derived cell lines with unique genetic lesions distinct from VHL deficiency, EA cytotoxicity paralleled sensitivity to 2-deoxy-D-glucose (2-DG), itself an indicator of glucose dependence (see Table 1). In each case, correction of the unique genetic lesion in isogenic cell lines abrogated both EA sensitivity and 2-DG cytotoxicity. Nontumorigenic cell lines derived from normal kidney epithelium were resistant to both EA and 2-DG. Importantly, however, nontumorigenic HEK293 cells can be made sensitive to EA by exogenous expression of both PKCθ and HSF1.

Although the crystal structure of EA bound to PKCθ will be necessary to unambiguously identify its binding domain, competition binding experiments with the fluorescent phorbol ester SAPD suggest that EA binds within or adjacent to the C1 domain of PKCθ. Because EA is not able to compete with SAPD binding to PKCδ, and because EA is structurally dissimilar from either phorbol esters or DAG, it is likely that EA has binding requirements that are only met in PKCθ.

Because of the lack of selectivity of most PKC modulators, the unique role of PKCθ in cancer biology has remained unclear. Here, we have identified PKCθ as an important pharmacologic target in glucose-dependent tumor cells. Kim and collaborators first identified a link between PKCθ and insulin resistance when they demonstrated that PKCθ knockout mice were protected from developing fat-induced insulin resistance (Kim et al., 2004). We confirmed the association of PKCθ with insulin resistance in tumor cells by showing that selective activation of PKCθ disrupts insulin signaling to AKT and induces an insulin-resistant phenotype reminiscent of that caused in skeletal muscle by a high fat diet and observed in patients with type 2 diabetes (Samuel and Shulman, 2012).

We suspect that the lack of hyperglycemia in EA-treated mice is due to increased HSP70 levels because elevated HSP70 has been shown to enhance insulin sensitivity (Chung et al., 2008; Kavanagh et al., 2011). Because EA promoted increased HSP70 expression in tumor xenografts and in tumor cells in vitro, we examined the possible impact of EA on HSF1, a transcriptional regulator of *HSP70* and a protein frequently upregulated in cancer (Whitesell and Lindquist, 2009; Santagata et al., 2011). As discussed earlier, HSF1 enhances tumor glucose dependence and the transcription factor, although not transforming on its own, is considered to be a critical contributor to tumor cell survival (Dai et al., 2007; Solimini et al., 2007). Recently, HSF1 has been reported to transcriptionally regulate a number of genes not involved in the heat shock response of

normal cells but which are commonly upregulated in cancer cells (Mendillo et al., 2012). Thus, inhibition of HSF1 is predicted to be of therapeutic value in cancer (Whitesell and Lindquist, 2009).

Unexpectedly, although EA stimulates HSF1 transcriptional activity, we found this to be a prerequisite for EA cytotoxicity. Thus, we propose that EA is synthetically lethal for tumor cells that simultaneously express PKCθ and are addicted to HSF1. PKCθ activates HSF1 by phosphorylating serine 333 in the stress responsive regulatory domain. Mutation of this residue to a non-phosphorylatable (S333A) or phosphomimetic (S333E) amino acid markedly affects the interaction of HSF1 with HSP90. Because dissociation of HSF1 from HSP90 is a prerequisite for HSF1 activation and nuclear translocation (Anckar and Sistonen, 2011), these data provide a mechanistic basis to explain PKCθ-dependent activation of HSF1 by EA. Importantly, EA sensitivity is strongly correlated with glucose dependence and is most pronounced when glucose availability is limiting.

In summary, our data show that PKCθ-mediated induction of insulin resistance occurring simultaneously with PKCθ-mediated HSF1 activation is responsible for EA cytotoxicity. PKCθ thus represents a unique molecular target for HSF1-addicted glycolytic tumors, and EA provides a template for designing effective PKCθ-activating drugs.

EXPERIMENTAL PROCEDURES

Cell Lines and Cell Culture

The sporadic VHL-deficient kidney tumor cell line 786-0 (Williams et al., 1978), the prostate cancer cell line PC3 (Kaighn et al., 1979), the breast cancer cell line SKBr3 (Fogh and Trempe, 1975), the normal kidney cell line HK2 (Ryan et al., 1994), and HEK293T, an embryonic kidney epithelial cell line (Pear et al., 1993), were all purchased from ATCC. UOK262, UOK262WT, UOK257, UOK257-2 (WT), and 786/VHL were established within the Urologic Oncology Branch. UOK262 is a kidney cancer cell line derived from a metastasis that is deficient in fumarate hydratase (FH) (Yang et al., 2010). UOK262WT was established by stably transfecting UOK262 with a functional *FH* gene (Tong et al., 2011) and is therefore considered to be "molecularly restored." UOK257 is a folliculin (FLCN)-deficient kidney tumor cell line derived from human renal carcinoma of an individual with Birt-Hogg-Dubé (BHD) syndrome and its molecularly restored counterpart UOK257-2 (WT) was established by stably transfecting UOK257 with *FLCN* (Yang et al., 2008; Hong et al., 2010). The stably *VHL*-transfected 786-0 (786/VHL) cell line has been described previously (Tong et al., 2011). Cells were cultured in Dulbecco's modified Eagle's medium (DMEM) high glucose without sodium pyruvate (Cellgro, Herndon, VA, USA) or in RPMI-1640 (PC3 only) supplemented with 10% fetal bovine serum (Invitrogen, Grand Island, NY, USA). Viability experiments were performed in serum-free media.

Reagents

EA was generously supplied by R. Akee of the Natural Products Support Group (Developmental Therapeutics Program, National Cancer Institute, Frederick National Laboratory, Frederick, MD, USA). Complete mini protease inhibitor cocktail tablets were purchased from Roche (Indianapolis, IN, USA). The siRNAs for PKC-α and -ζ were purchased from OriGene (Rockville, MD, USA). The siRNAs for PKC-θ, -δ, and -ε were from Santa Cruz Biotechnology (Santa Cruz, CA, USA). Purified HSF1, PKC-θ, -α, and -δ were purchased from EnzoLife Sciences (Farmingdale, NY, USA).

Prediction of EA Targets

Metadrug (Genego, Carlsbad, CA, USA) is a systems pharmacology platform using QSAR modeling to analyze and compare biological effects of small molecules. We used it to predict potential targets for EA (see a complete list of predicted targets in Table S1).

Nonradioactive PKC Kinase Assay

PKC kinase activity of cell lysates was measured using the pan-PKC activity assay from EnzoLife Sciences, following the manufacturer's recommendations. Briefly, cells were lysed in TNESV lysis buffer (50 mM Tris, 1% Nonidet P-40, 2 mM EDTA, 100 mM NaCl, and 2 mM Na_3VO_4). After 15 min of centrifugation (13, 200 rpm, 4°C), clarified supernatant was incubated with 10 μM EA in the kinase buffer provided by the manufacturer (1 hr at 30°C with 10 μM ATP). The reaction was stopped by emptying the wells prior to measuring the phosphorylation of a PKC substrate by spectrophotometry. PKCα, -δ, and -θ kinase assays were performed in a similar manner using 5 ng of purified PKC proteins instead of cell lysate (incubation for 1 hr at 30°C with 10 μM ATP). Kinase activity was also assessed by incubating purified PKCθ (10 ng) with purified IRS1 (20 ng) in presence of increasing concentrations of EA (incubation for 1 hr at 30°C with 10 μM ATP). The reaction was stopped by adding denaturing sample buffer, and phosphorylation of IRS1 on S1101 was assessed by immunoblot analysis.

Radioactive In Vitro Kinase Assay

Purified IRS1 (50 ng) or HSF1 (50 ng) was incubated with purified PKCθ (50 ng) in presence or absence of EA (100 nM). Reactions were initiated by the addition of 10 μM nonradioactive ATP and 6 μCi (0.2 μM) of [^{32}P]-ATP and incubated at 30°C for 30 min with periodic mixing. Proteins in the kinase reactions were separated by SDS-PAGE and transferred to PVDF membrane. Phosphorylation of IRS1 or HSF1 was assessed by radiography of PVDF membranes. IRS1 or HSF1 were immunoblotted to ensure equal loading.

Phorbol Ester Competition Binding Assay

The fluorescent phorbol ester sapintoxin D (SAPD, 2 μM; Santa Cruz) (Taylor et al., 1981) was incubated with purified PKC proteins (5 ng) after preincubation for 20 min with EA (1 μM) or DMSO. Fluorescence of SAPD is shifted from 455 to 420 nm when it is bound to PKC. Therefore, we monitored fluorescence emission at 420 nm to determine SAPD binding to PKC proteins (Das et al., 2004).

Glucose Uptake Assay

Glucose uptake was measured using a fluorescent nonmetabolizable D-glucose analog 2-[*N*-(7-nitrobenz-2-oxa-1,3-diazol-4-yl) amino]-2-deoxy-D-glucose (2-NBDG; Cayman Chemicals, Ann Arbor, MI) as previously described (O'Neil et al., 2005), with the following modifications. Five thousand cells were plated in black-well 96-well plates. After treatment as indicated (3 hr), cells were incubated for 20 min in KREB buffer containing 1g/l glucose in presence or absence of 20 μM 2-NBDG. Cells were then washed three times for 5 min with PBS to remove all residual extracellular 2-NBDG. The amount of 2-NBDG imported into the cells was measured by assessing fluorescence at 488 nm. The Glut 1 inhibitor fasentin (50 μM; Sigma-Aldrich, St. Louis, MO) was used as a positive control.

HSP70 Secretion

Plasma HSP70 in tumor-bearing mice was assessed using an ELISA kit purchased from EnzoLife Sciences and following the manufacturer's protocol. Blood was collected 4 hr after EA or vehicle (PBS/DMSO, 1/1) injection.

HSF1 Transcriptional Activity

Cellular HSF1 transcriptional activity was measured using a green fluorescent protein (GFP)-tag HSE promoter reporter (generously provided by Dr. Luke Whitesell, Whitehead Institute, Cambridge, MA, USA). Twenty-four hours prior to analysis, 5,000 786-0 cells were plated in 96-well black-view plates. While still in suspension, cells were transfected with the reporter plasmid (1 μg DNA) using lipofectamine LTX (Invitrogen) and following the manufacturer's protocol. To avoid potential interference of the phenol red from the media with the GFP reading, phenol red-free DMEM (high glucose and without sodium pyruvate) was used instead of regular DMEM. The following day, 786-0 cells were treated as described with EA 6 hr prior to measure the amount of GFP produced using a spectrophotometer (488 nm). For HSF1 silencing experiments, 786-0 cells were transfected with 14 μg of shRNA to HSF1 in 6-well plates using lipofectamine LTX (Invitrogen) 2 days prior to plating into 96-well black-view plates. Nuclear translocation of HSF1 was visualized by immunofluorescence. Three thousand 786-0 cells were plated in 2-well

chamber-slides (Nunc/Sigma-Aldrich) and treated for 1 hr with EA (1 μM) before fixation with 4% paraformaldehyde. Cells were blocked 1 hr with BSA (3%) and permeabilized with Triton (0.5%). HSF1 antibody was incubated overnight at 4°C in a humidified atmosphere. After three washes with TBST buffer, slides were incubated 1 hr with secondary antibody coupled to Alexa455, washed, and mounted. DAPI (Cell Signaling Technology, Danvers, MA, USA) was used to visualize cell nuclei. Pictures were taken with a confocal microscope (Zeiss NLO510).

Xenograft Tumor Studies

Animal experiments were carried out following the ethical guidelines of the National Cancer Institute and using an animal protocol approved by the National Institutes of Health Animal Care Facility. Ten million 786-0 or one million PC3 cells were implanted subcutaneously on the left flanks of twenty 7-week-old female nude (Nu/Nu) mice (strain code 088; Charles River, Wilmington, MA, USA). After 1–4 weeks (depending on the cell line), tumors reached an average volume of 100–150 mm^3. Tumor take for both 786-0 and PC3 xenografts was 100%; however, to maintain homogenous group sizes, only 16 mice out of the 20 were used. Mice were then randomly separated in two groups of eight mice with comparable tumor volumes and treated six times a week (daily except Sunday) intraperitoneally with either EA at 5 mg/kg or vehicle (PBS/DMSO, 1/1). Food and water were available ad libitum. Tumors were measured throughout the duration of the experiment using calipers and tumor volumes were estimated using the formula $(l \times w^2)/2$. At the end of the experiment, blood was collected, and tumors were surgically excised and frozen for further analysis. Animal experiments were performed twice with eight animals per group each time.

Statistics

Unless specified, all values are expressed as the mean ± standard error. Values were compared using the Student-Newman-Keul's test. $p < 0.05$ was considered significant.

SUPPLEMENTAL INFORMATION

Supplemental Information includes one table, four figures, and Supplemental Experimental Procedures and can be found with this article online at http://dx.doi.org/10.1016/j.ccr.2012.12.007.

ACKNOWLEDGMENTS

We thank Drs. S. Calderwood (Harvard University, Cambridge, MA) and L. Whitesell (Whitehead Institute, Cambridge, MA) for generously providing reagents. We thank Dr. P.L. Nagy (N-Gene Research Laboratories, Budapest, Hungary) for generously providing BGP-15. We thank Drs. N. Kedei and P. Blumberg (National Cancer Institute, Bethesda, MD) and P. Csermely (Semmelweis University, Budapest, Hungary) for helpful discussions. This research was supported with funds provided by the Intramural Research Program of the National Cancer Institute.

Received: June 4, 2012
Revised: October 19, 2012
Accepted: December 18, 2012
Published: January 24, 2013

REFERENCES

Anckar, J., and Sistonen, L. (2011). Regulation of HSF1 function in the heat stress response: implications in aging and disease. Annu. Rev. Biochem. *80*, 1089–1115.

Barbieri, M., Bonafè, M., Franceschi, C., and Paolisso, G. (2003). Insulin/IGF-I-signaling pathway: an evolutionarily conserved mechanism of longevity from yeast to humans. Am. J. Physiol. Endocrinol. Metab. *285*, E1064–E1071.

Chan, D.A., Sutphin, P.D., Nguyen, P., Turcotte, S., Lai, E.W., Banh, A., Reynolds, G.E., Chi, J.T., Wu, J., Solow-Cordero, D.E., et al. (2011). Targeting GLUT1 and the Warburg effect in renal cell carcinoma by chemical synthetic lethality. Sci. Transl. Med. *3*, 94ra70.

Chung, J., Nguyen, A.K., Henstridge, D.C., Holmes, A.G., Chan, M.H., Mesa, J.L., Lancaster, G.I., Southgate, R.J., Bruce, C.R., Duffy, S.J., et al. (2008). HSP72 protects against obesity-induced insulin resistance. Proc. Natl. Acad. Sci. USA *105*, 1739–1744.

Dai, C., Whitesell, L., Rogers, A.B., and Lindquist, S. (2007). Heat shock factor 1 is a powerful multifaceted modifier of carcinogenesis. Cell *130*, 1005–1018.

Das, J., Addona, G.H., Sandberg, W.S., Husain, S.S., Stehle, T., and Miller, K.W. (2004). Identification of a general anesthetic binding site in the diacylglycerol-binding domain of protein kinase Cdelta. J. Biol. Chem. *279*, 37964–37972.

Fogh, J., and Trempe, G. (1975). Human tumor cells in vitro (New York: Plenum Publishing), pp. 115–141.

Gallagher, E.J., and LeRoith, D. (2011). Minireview: IGF, Insulin, and Cancer. Endocrinology *152*, 2546–2551.

Gambhir, S.S. (2002). Molecular imaging of cancer with positron emission tomography. Nat. Rev. Cancer *2*, 683–693.

Griffin, M.E., Marcucci, M.J., Cline, G.W., Bell, K., Barucci, N., Lee, D., Goodyear, L.J., Kraegen, E.W., White, M.F., and Shulman, G.I. (1999). Free fatty acid-induced insulin resistance is associated with activation of protein kinase C theta and alterations in the insulin signaling cascade. Diabetes *48*, 1270–1274.

Griner, E.M., and Kazanietz, M.G. (2007). Protein kinase C and other diacylglycerol effectors in cancer. Nat. Rev. Cancer *7*, 281–294.

Hamanaka, R.B., and Chandel, N.S. (2012). Targeting glucose metabolism for cancer therapy. J. Exp. Med. *209*, 211–215.

Hargitai, J., Lewis, H., Boros, I., Rácz, T., Fiser, A., Kurucz, I., Benjamin, I., Vígh, L., Pénzes, Z., Csermely, P., and Latchman, D.S. (2003). Bimoclomol, a heat shock protein co-inducer, acts by the prolonged activation of heat shock factor-1. Biochem. Biophys. Res. Commun. *307*, 689–695.

Hong, S.B., Oh, H., Valera, V.A., Stull, J., Ngo, D.T., Baba, M., Merino, M.J., Linehan, W.M., and Schmidt, L.S. (2010). Tumor suppressor FLCN inhibits tumorigenesis of a FLCN-null renal cancer cell line and regulates expression of key molecules in TGF-beta signaling. Mol. Cancer *9*, 160.

Kaighn, M.E., Narayan, K.S., Ohnuki, Y., Lechner, J.F., and Jones, L.W. (1979). Establishment and characterization of a human prostatic carcinoma cell line (PC-3). Invest. Urol. *17*, 16–23.

Kavanagh, K., Flynn, D.M., Jenkins, K.A., Zhang, L., and Wagner, J.D. (2011). Restoring HSP70 deficiencies improves glucose tolerance in diabetic monkeys. Am. J. Physiol. Endocrinol. Metab. *300*, E894–E901.

Kim, J.K., Fillmore, J.J., Sunshine, M.J., Albrecht, B., Higashimori, T., Kim, D.W., Liu, Z.X., Soos, T.J., Cline, G.W., O'Brien, W.R., et al. (2004). PKC-theta knockout mice are protected from fat-induced insulin resistance. J. Clin. Invest. *114*, 823–827.

Leto, D., and Saltiel, A.R. (2012). Regulation of glucose transport by insulin: traffic control of GLUT4. Nat. Rev. Mol. Cell Biol. *13*, 383–396.

Li, Y., Soos, T.J., Li, X., Wu, J., Degennaro, M., Sun, X., Littman, D.R., Birnbaum, M.J., and Polakiewicz, R.D. (2004). Protein kinase C Theta inhibits insulin signaling by phosphorylating IRS1 at Ser(1101). J. Biol. Chem. *279*, 45304–45307.

Literáti-Nagy, B., Kulcsár, E., Literáti-Nagy, Z., Buday, B., Péterfai, E., Horváth, T., Tory, K., Kolonics, A., Fleming, A., Mandl, J., and Korányi, L. (2009). Improvement of insulin sensitivity by a novel drug, BGP-15, in insulin-resistant patients: a proof of concept randomized double-blind clinical trial. Horm. Metab. Res. *41*, 374–380.

Luo, J.H., and Weinstein, I.B. (1993). Calcium-dependent activation of protein kinase C. The role of the C2 domain in divalent cation selectivity. J. Biol. Chem. *268*, 23580–23584.

Marsland, B.J., and Kopf, M. (2008). T-cell fate and function: PKC-theta and beyond. Trends Immunol. *29*, 179–185.

Mendillo, M.L., Santagata, S., Koeva, M., Bell, G.W., Hu, R., Tamimi, R.M., Fraenkel, E., Ince, T.A., Whitesell, L., and Lindquist, S. (2012). HSF1 drives a transcriptional program distinct from heat shock to support highly malignant human cancers. Cell *150*, 549–562.

Min, J.N., Huang, L., Zimonjic, D.B., Moskophidis, D., and Mivechi, N.F. (2007). Selective suppression of lymphomas by functional loss of Hsf1 in a p53-deficient mouse model for spontaneous tumors. Oncogene *26*, 5086–5097.

Nelson, T.J., Sun, M.K., Hongpaisan, J., and Alkon, D.L. (2008). Insulin, PKC signaling pathways and synaptic remodeling during memory storage and neuronal repair. Eur. J. Pharmacol. *585*, 76–87.

O'Neil, R.G., Wu, L., and Mullani, N. (2005). Uptake of a fluorescent deoxyglucose analog (2-NBDG) in tumor cells. Mol. Imaging Biol. *7*, 388–392.

Pear, W.S., Nolan, G.P., Scott, M.L., and Baltimore, D. (1993). Production of high-titer helper-free retroviruses by transient transfection. Proc. Natl. Acad. Sci. USA *90*, 8392–8396.

Pirkkala, L., Nykänen, P., and Sistonen, L. (2001). Roles of the heat shock transcription factors in regulation of the heat shock response and beyond. FASEB J. *15*, 1118–1131.

Ratnayake, R., Covell, D., Ransom, T.T., Gustafson, K.R., and Beutler, J.A. (2009). Englerin A, a selective inhibitor of renal cancer cell growth, from Phyllanthus engleri. Org. Lett. *11*, 57–60.

Ryan, M.J., Johnson, G., Kirk, J., Fuerstenberg, S.M., Zager, R.A., and Torok-Storb, B. (1994). HK-2: an immortalized proximal tubule epithelial cell line from normal adult human kidney. Kidney Int. *45*, 48–57.

Samuel, V.T., and Shulman, G.I. (2012). Mechanisms for insulin resistance: common threads and missing links. Cell *148*, 852–871.

Santagata, S., Hu, R., Lin, N.U., Mendillo, M.L., Collins, L.C., Hankinson, S.E., Schnitt, S.J., Whitesell, L., Tamimi, R.M., Lindquist, S., and Ince, T.A. (2011). High levels of nuclear heat-shock factor 1 (HSF1) are associated with poor prognosis in breast cancer. Proc. Natl. Acad. Sci. USA *108*, 18378–18383.

Solimini, N.L., Luo, J., and Elledge, S.J. (2007). Non-oncogene addiction and the stress phenotype of cancer cells. Cell *130*, 986–988.

Taylor, S.E., Gafur, M.A., Choudhury, A.K., and Evans, F.J. (1981). Sapintoxin A, a new biologically active nitrogen containing phorbol ester. Experientia *37*, 681–682.

Tong, W.H., Sourbier, C., Kovtunovych, G., Jeong, S.Y., Vira, M., Ghosh, M., Romero, V.V., Sougrat, R., Vaulont, S., Viollet, B., et al. (2011). The glycolytic shift in fumarate-hydratase-deficient kidney cancer lowers AMPK levels, increases anabolic propensities and lowers cellular iron levels. Cancer Cell *20*, 315–327.

Trepel, J., Mollapour, M., Giaccone, G., and Neckers, L. (2010). Targeting the dynamic HSP90 complex in cancer. Nat. Rev. Cancer *10*, 537–549.

Vander Heiden, M.G., Cantley, L.C., and Thompson, C.B. (2009). Understanding the Warburg effect: the metabolic requirements of cell proliferation. Science *324*, 1029–1033.

Whitesell, L., and Lindquist, S. (2009). Inhibiting the transcription factor HSF1 as an anticancer strategy. Expert Opin. Ther. Targets *13*, 469–478.

Williams, R.D., Elliott, A.Y., Stein, N., and Fraley, E.E. (1978). In vitro cultivation of human renal cell cancer. II. Characterization of cell lines. In Vitro *14*, 779–786.

Yang, Y., Padilla-Nash, H.M., Vira, M.A., Abu-Asab, M.S., Val, D., Worrell, R., Tsokos, M., Merino, M.J., Pavlovich, C.P., Ried, T., et al. (2008). The UOK 257 cell line: a novel model for studies of the human Birt-Hogg-Dubé gene pathway. Cancer Genet. Cytogenet. *180*, 100–109.

Yang, Y., Valera, V.A., Padilla-Nash, H.M., Sourbier, C., Vocke, C.D., Vira, M.A., Abu-Asab, M.S., Bratslavsky, G., Tsokos, M., Merino, M.J., et al. (2010). UOK 262 cell line, fumarate hydratase deficient (FH-/FH-) hereditary leiomyomatosis renal cell carcinoma: in vitro and in vivo model of an aberrant energy metabolic pathway in human cancer. Cancer Genet. Cytogenet. *196*, 45–55.

Zou, J., Guo, Y., Guettouche, T., Smith, D.F., and Voellmy, R. (1998). Repression of heat shock transcription factor HSF1 activation by HSP90 (HSP90 complex) that forms a stress-sensitive complex with HSF1. Cell *94*, 471–480.